Paper No. 264. (quote when citing this article)
Eleventh World Conference on Earthquake Engineering
ISBN: 0 08 042822 3

SIMPLE MODEL FOR SIMULATING HYSTERETIC BEHAVIOR INVOLVING SIGNIFICANT STRAIN HARDENING

T. AKAZAWA, M. NAKASHIMA AND O. SAKAGUCHI

Geo-Research Institute, Osaka Soil Test Laboratory
3-1-23 Nishihonmachi, Nishi-ku, Osaka 550 JAPAN
Disaster Prevention Research Institute, Kyoto University
Gokasho, Uji, Kyoto 611 JAPAN
Faculty of Science and Engineering, Kinki University
3-4-1 Kowakae, Higashiosaka, Osaka 577 JAPAN

ABSTRACT

This paper proposes a simple model that can simulate the hysteretic behavior of shear panels made of low-yield steel, which exhibits significant strain-hardening under load reversals. The model is based on the Ramberg-Osgood model, and combine kinematic and isotropic hardening in a linear manner by the introduction of a weighting coefficient. The accuracy of the model is demonstrated by comparing hysteresis curves obtained from this model with experimental hysteresis curves.

KEYWORDS

hysteretic damper; low-yield steel; shear panel; kinematic hardening; isotropic hardening; bilinear model, Ramberg-Osgood model.

INTRODUCTION

Background of this paper is an increasing use of hysteretic dampers in structures for more positive vibration control. To enhance the damping, low-yield steel is often used for dampers' materials. According to previous investigations (for example, Tamai *et al.* 1991, Izumi *et al.* 1992, Nakashima *et al.* 1994), dampers made of low-yield steel are very ductile, thus effective for energy dissipation, but are involved with significant strain hardening. The objective of this study is to propose a simple analytical model that can simulate the hysteretic behavior of hysteretic dampers made of low-yield steel. In formulating the model, the following two principles were kept in mind: (1) the model can simulate reasonably the significant strain-hardening observed from the experiment and (2) the model is sufficiently simple that they can readily be incorporated into time-history dynamic response analysis of structural systems. The model has its basis on the I-K bilinear model that had been devised originally by Yamada and Tsuji (1965), and basic rules of the Ramberg-Osgood functions (Jennings, 1964) are adopted.

I-K BILINEAR MODEL

The I-K bilinear model is a direct and simple combination of the isotropic hardening model proposed by Hill (1950) and the kinematic hardening model proposed by Prager (1956), and a parameter (β) that specifies the proportion of the kinematic and isotropic hardening in a linear manner is included. The basic rules used in this model are visually described in Fig.1 and full details are given in Nakashima *et al.* (1995). The key for programming this model is the fact that there is a stress bound within which only kinematic hardening takes place. This bound, called the kinematic hardening bound, has an upper and a lower limit stress, whose absolute values are the same and correspond to the maximum stress experienced in the previous loading history. Furthermore, this bound never shrinks but remains unchanged unless the stress goes beyond the present bound. For example, in the state shown in Fig.1(d), the magnitude of the limit stress is: ($\bar{\sigma}_0 + |\Delta\sigma_1|$), and, as

long as the stress obtained remains between $-(\bar{\sigma}_0+|\Delta\sigma_1|)$ and $+(\bar{\sigma}_0+|\Delta\sigma_1|)$, there is no isotropic hardening, and the kinematic hardening rules can be applied simply. Only when the stress exceeds the bound, the rules need to be modified. In reference to Fig.1(e), two modifications are needed, one for the expansion of the elastic range to $\bar{\sigma}_2$, and the other for the expansion of the kinematic hardening limit to $-(\bar{\sigma}_0+|\Delta\sigma_1|+|\Delta\sigma_2|)$ and $(\bar{\sigma}_0+|\Delta\sigma_1|+|\Delta\sigma_2|)$.

In order to examine how accurately the model can simulate the hysteretic behavior involving significant hardening, the model was applied for the test results obtained earlier for a shear panel damper with a 9 mm thick plate and subjected to repeated cyclic loading (Nakashima, 1995). Comparison was made for hysteresis loops up to the drift angle of 0.0114 (1/88). In reference to the test data, four parameters included in the I-K bilinear model, i.e., the initial elastic stiffness (K), the initial yield stress ($\bar{\sigma}_0$), the reduced stiffness (θK), and the strain-hardening parameter (β) were determined to be 55.0 GPa, 54.3 MPa, 0.015 and 0.85, respectively. Figure 2 compares the analytically obtained hysteresis curves with the experimental curves, demonstrating satisfactory correlation between the two and the ability of this model to trace hardening behavior. Because of the blinear nature of this model, however, the model fails in simulating gradual degradation of stiffness appearing in the experimental hysteresis.

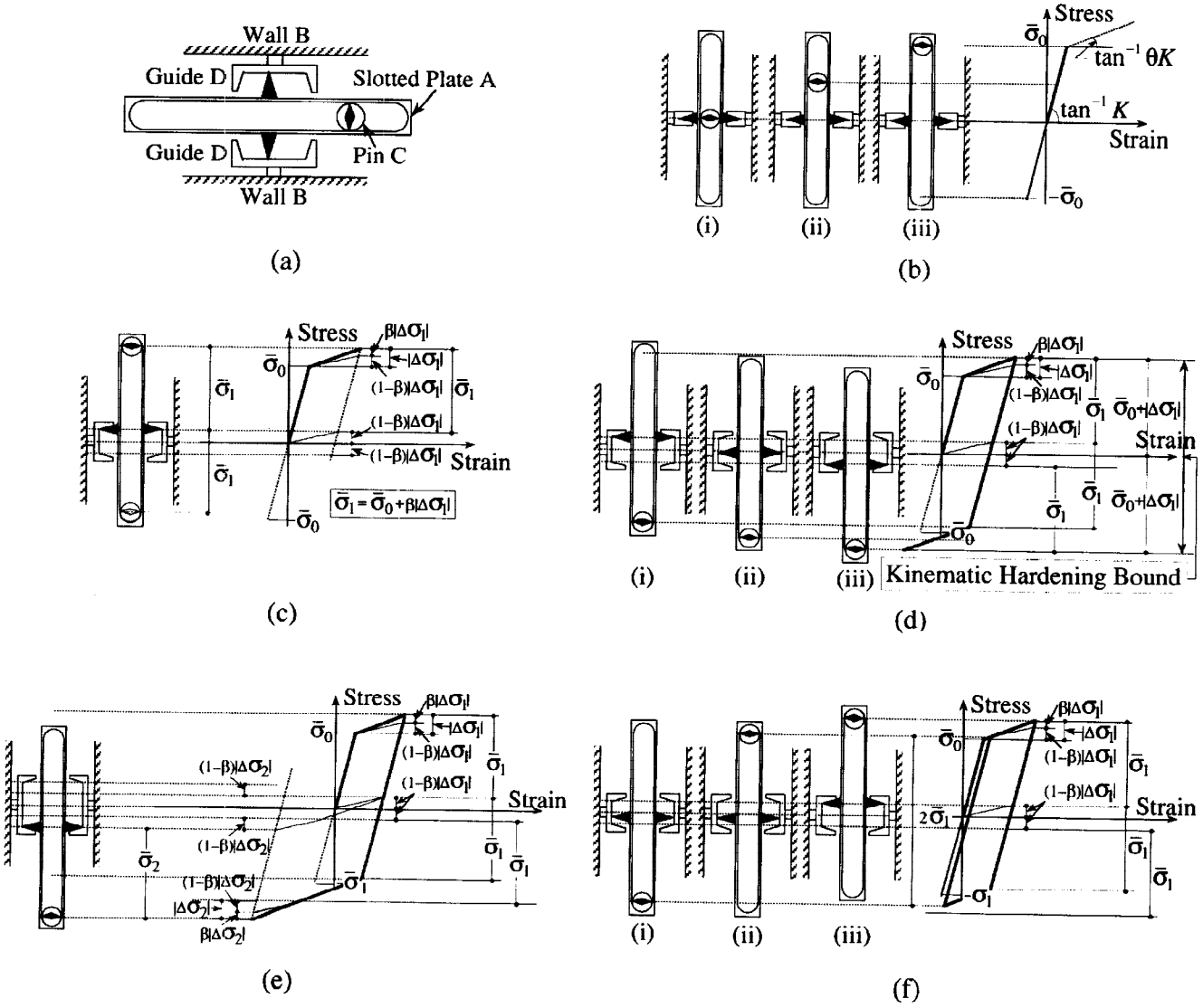

Fig.1 Formulation of I-K Biliner Model: (a)Concept of I-K Bilinear Model: (b)Initial Elastic Behavior in I-K Bilinear Model [(i)Original State; (ii)Initial Elastic Loading; (iii)Initial Yielding]: (c)Initial Inelastic Excursion in I-K Bilinear Model: (d)Unloading and Reloading in Opposite Direction After Initial Inelastic Excursion in I-K Bilinear Model [(i)Elastic Unloading and Reloading; (ii)Kinematic Hardening; (iii)Kinematic Hardening Bound]: (e)Isotropic Hardening During Loading in Opposite Direction in I-K Bilinear Model: (f)Load Reversal and Reloading for Second Time in I-K Bilinear Model [(i)Initiation of Unloading; (ii)Yielding; (iii)Kinematic Hardening]

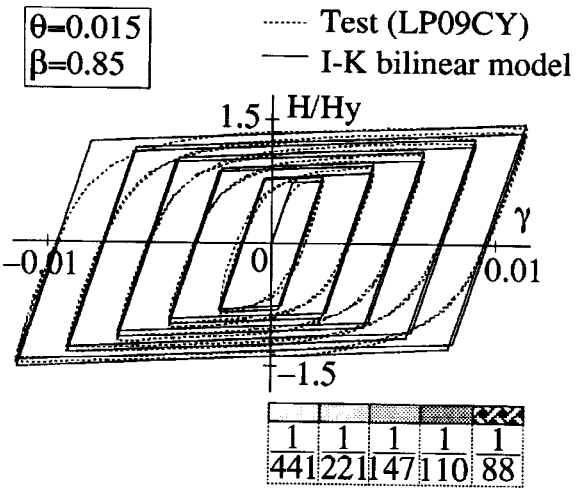

Fig.2 Comparison Between Experimental Hysteresis and Hysteresis Obtained from I-K Bilinear Model (from Test LP09CY)

COMBINED I-K AND RAMBERG-OSGOOD MODEL

Conceptually, kinematic hardening is characterized by the shift of the neutral position, whereas isotropic hardening is characterized by enlargement of hysteresis, and the I-K bilinear model proportions these two types of hardening in a linear manner by the introduction of a weighting coefficient designated as β. As described in the previous section, the model assumes that isotropic hardening takes place and accordingly the kinematic hardening bound enlarges only when the stress exceeds the present kinematic hardening bound. It was found that these simple rules embedded in this model can readily be incorporated into hysteresis models other than the bilinear model. In what follows, a model based upon the Ramberg-Osgood functions, referred to as the RO model in this paper, is chosen, and a modified version of the RO model (referred to as the I-K RO model), in which a combined isotropic and kinematic hardening is taken into account, is developed.

Ramberg-Osgood Model

The RO model is often used for its capacity to trace gradual degradation of stiffness. The model consists of a skeleton curve and a family of hysteresis curves as shown in Fig.3(a). The skeleton curve is expressed as:

$$\frac{\varepsilon}{\bar{\varepsilon}_0} = \frac{\sigma}{\bar{\sigma}_0}\left(1 + \alpha\left|\frac{\sigma}{\bar{\sigma}_0}\right|^{\eta-1}\right) \tag{1}$$

where σ, $\bar{\sigma}_0$, ε, and $\bar{\varepsilon}_0$, are the stress, yield stress, strain, and yield strain, respectively, and α and η are the two coefficients that specify the shape of the curve. With the initial stiffness given as K, the relationship between $\bar{\sigma}_0$ and $\bar{\varepsilon}_0$ is:

$$\bar{\sigma}_0 = K\,\bar{\varepsilon}_0 \tag{2}$$

A hysteresis curve is given as:

$$\frac{\varepsilon - \varepsilon_0}{2\bar{\varepsilon}_0} = \frac{\sigma - \sigma_0}{2\bar{\sigma}_0}\left(1 + \alpha\left|\frac{\sigma - \sigma_0}{2\bar{\sigma}_0}\right|^{\eta-1}\right) \tag{3}$$

where σ_0 and ε_0 indicate the coordinates of the origin of the curve, i.e., the point of most recent load reversal. The hysteresis curve is the same in shape as the skeleton curve but enlarged twice for both the vertical (stress) and horizontal (strain) axes. Furthermore, the origin is shifted to the point of most recent load reversal. The same explanation is applicable for the bilinear model as shown in Fig.3(b), in which the skeleton curve has an elastic stiffness K, yield stress $\bar{\sigma}_0$, and stiffness of the second branch θK. A hysteresis curve also has K and θK for the stiffnesses, indicating that the skeleton and hysteresis curves have the identical shape, and its elastic range is enlarged twice. This analogy forms a basis for the following formulation.

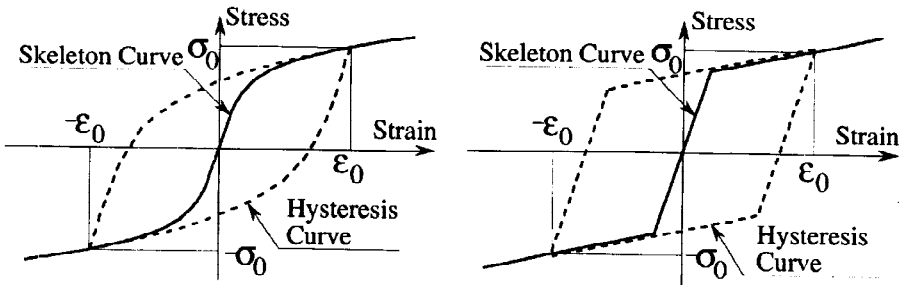

Fig.3 Concept of RO Model and Bilinear Model:
(a) RO Model; and (b) Bilinear Model

Formulation of I-K RO Model

Figure 4(a) illustrates the initial loading from the unloaded state. Here the initial yield force of the model ($\bar{\sigma}_0$) is taken to specify the initial kinematic hardening bound, i.e., the bound enclosed between $-\bar{\sigma}_0$ and $+\bar{\sigma}_0$. The skeleton curve in this range is simply given by (1). As long as the stress stays within the bound, no isotropic hardening occurs, and succeeding loading, unloading, and reloading follow the rules given in the original RO model. Thus, the hysteresis curve is given by (3). Figure 4(b) shows the state where the structure is loaded beyond $\bar{\sigma}_0$ and reaches Point A, whose coordinates are designated as (ε_1, σ_1). The stress increment beyond the initial kinematic hardening bound is given as:

$$\Delta\sigma_1 = \sigma_1 - \bar{\sigma}_0 \tag{4}$$

When unloaded at Point A, the elastic range is taken to enlarge by $\beta|\Delta\sigma_1|$ according to the rule described for the I-K bilinear model. In the I-K RO model, this condition is allowed for by changing the yield stress of the RO model from $\bar{\sigma}_0$ to $\bar{\sigma}_1$ [$=(\bar{\sigma}_0 + \beta|\Delta\sigma_1|)$] and corresponding yield strain from $\bar{\varepsilon}_0$ to $\bar{\varepsilon}_1$ ($=\bar{\sigma}_1/K$). Thus, the hysteresis curve for unloading from Point A is:

$$\frac{\varepsilon-\varepsilon_1}{2\bar{\varepsilon}_1} = \frac{\sigma-\sigma_1}{2\bar{\sigma}_1}\left(1+\alpha\left|\frac{\sigma-\sigma_1}{2\bar{\sigma}_1}\right|^{\eta-1}\right) \tag{5}$$

According to the RO model, when the hysteresis curve reaches the skeleton curve, the path changes and travels on the skeleton curve for further loading [Fig.3(a)]. To account for this rule in the proposed model, a new skeleton curve is defined. Assuming that the skeleton curve has the same shape as the hysteresis curve with halved coordinates, one can obtain the following expression for the new skeleton curve:

$$\frac{\varepsilon-o_{\varepsilon 1}}{\bar{\varepsilon}_1} = \frac{\sigma-o_{\sigma 1}}{\bar{\sigma}_1}\left(1+\alpha\left|\frac{\sigma-o_{\sigma 1}}{\bar{\sigma}_1}\right|^{\eta-1}\right) \tag{6}$$

Here, ($o_{\varepsilon 1}$, $o_{\sigma 1}$) indicates the coordinates of the origin of the new skeleton curve [Point O_1 in Fig.4(b)]. Assuming that the skeleton curve also goes through Point A and knowing that the yield stress is now increased by $\beta|\Delta\sigma_1|$, one can readily obtain:

$$o_{\sigma 1} = -\beta\Delta\sigma_1 \tag{7}$$

[Note that, in reference to Fig.4(b), $o_{\sigma 1}$ is negative, because $\Delta\sigma_1$ is positive.] Point B in Fig.4(b) denotes the intersection of the hysteresis curve with the skeleton curve in the opposite direction. Since Points A and B are situated skewed-symmetrically with respect to the origin (O_1), the stress at Point B (σ_B) is:

$$\sigma_B = 2o_{\sigma 1} - \sigma_1 \tag{8}$$

The hysteresis curve (5) should also passes through Point B, and substituting (8) into σ in (5) gives for the strain at Point B (ε_B) as:

$$\varepsilon_B = \frac{\sigma_B-\sigma_1}{\bar{\sigma}_1}\left(1+\alpha\left|\frac{\sigma_B-\sigma_1}{2\bar{\sigma}_1}\right|^{\eta-1}\right)\bar{\varepsilon}_1 + \varepsilon_1 \tag{9}$$

Since the skeleton curve (6) should also passes through Point B, inserting (7) to (9) into (6) leads to:

$$o_{\varepsilon 1} = -\frac{\sigma_B-o_{\sigma 1}}{\bar{\sigma}_1}\left(1+\alpha\left|\frac{\sigma_B-o_{\sigma 1}}{\bar{\sigma}_1}\right|^{\eta-1}\right)\bar{\varepsilon}_1 + \varepsilon_B \tag{10}$$

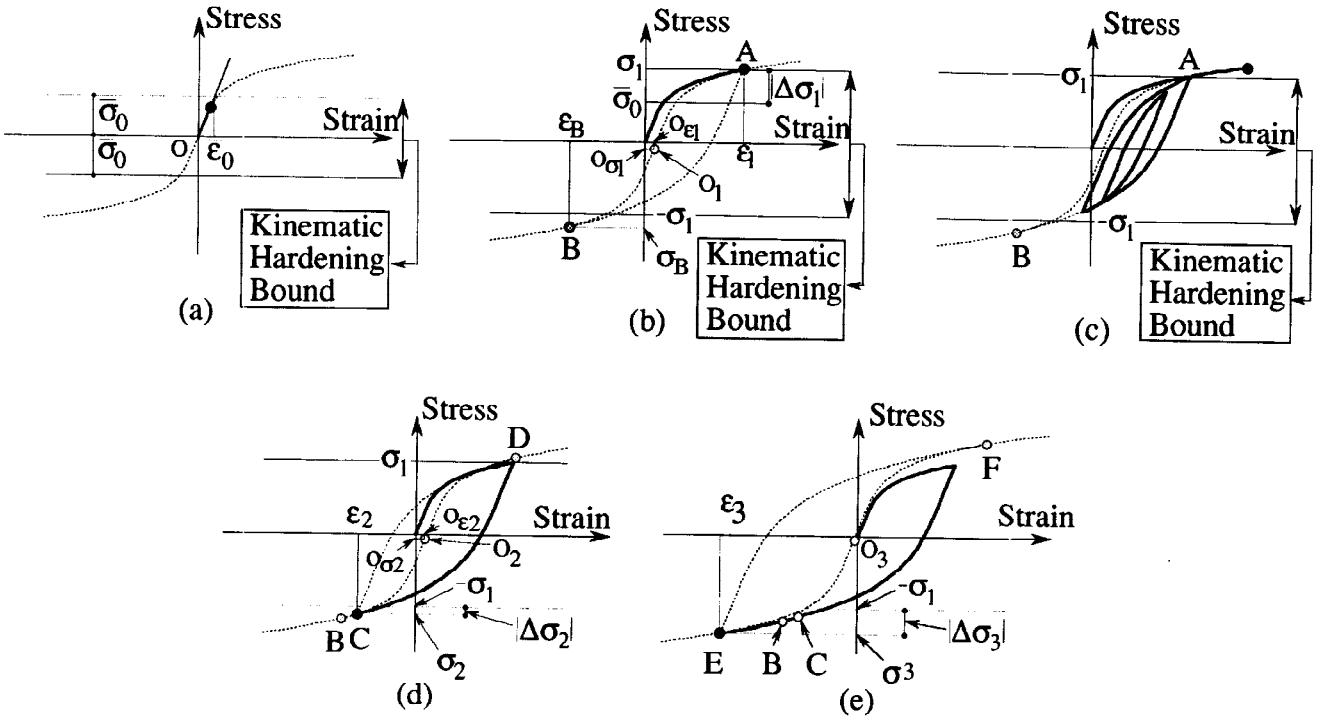

Fig.4 Rules Developed for I-K RO Model: (a) Initial Loading State; (b) Initial Isotropic Hardening; (c) Unloading and Reloading in Opposite Direction After Initial Isotropic Hardening; (d) Hardening During Loading in Opposite Direction Before Reaching Skeleton Curve; and (e) Hardening During Loading in Opposite Direction After Reaching Skeleton Curve

With $o_{\varepsilon 1}$ and $o_{\sigma 1}$ now defined by (10) and (7), the new skeleton curve (6) is defined uniquely. At the same time, the kinematic hardening bound is enlarged to $-\sigma_1$ and $+\sigma_1$. As long as the stress remains within the new kinematic hardening bound for the succeeding loading, the hysteresis rules of the RO model are applicable [Fig.4(c)]. When the structure is loaded beyond the kinematic hardening bound, isotropic hardening becomes involved again. Considered is a case shown in Fig.4(d), in which unloading takes place at Point C, whose coordinates are given (ε_2, σ_2), before reaching Point B, where the hysteresis curve is to intersect the skeleton curve. The stress increment from the kinematic hardening bound to the current state is:

$$\Delta\sigma_2 = \sigma_2 - (-\sigma_1) \tag{11}$$

[Note that, in reference to Fig.4(d), $\Delta\sigma_2$ is negative.] The yield stress is enlarged by $\beta|\Delta\sigma_2|$, with the new yield stress given as:

$$\bar{\sigma}_2 = \bar{\sigma}_1 + \beta|\Delta\sigma_2| \tag{12}$$

The new hysteresis curve, now moving to the positive direction in Fig.4(d), is given as:

$$\frac{\varepsilon - \varepsilon_2}{2\bar{\varepsilon}_2} = \frac{\sigma - \sigma_2}{2\bar{\sigma}_2}\left(1 + \alpha\left|\frac{\sigma - \sigma_2}{2\bar{\sigma}_2}\right|^{\eta-1}\right) \tag{13}$$

As in the case of Fig.4(b), the skeleton curve is defined as:

$$\frac{\varepsilon - o_{\varepsilon 2}}{\bar{\varepsilon}_2} = \frac{\sigma - o_{\sigma 2}}{\bar{\sigma}_2}\left(1 + \alpha\left|\frac{\sigma - o_{\sigma 2}}{\bar{\sigma}_2}\right|^{\eta-1}\right) \tag{14}$$

The ordinate of the new origin, $o_{\sigma 2}$, is given in a similar manner as in (7):

$$o_{\sigma 2} = o_{\sigma 1} - \beta\Delta\sigma_2 \tag{15}$$

[Note that, in reference to Fig.4(b), $\beta\Delta\sigma_2$ in (15) is negative.] The stress of Point D, the point of intersection between the hysteresis and skeleton curve on the opposite side, is also given as:

$$\sigma_D = 2o_{\sigma 2} - \sigma_B \tag{16}$$

Since the new hysteresis curve (13) passes through Point D, substitution of (16) to σ in (13) gives:

$$\varepsilon_D = \frac{\sigma_D - \sigma_2}{\bar{\sigma}_2}\left(1 + \alpha\left|\frac{\sigma_D - \sigma_2}{2\bar{\sigma}_2}\right|^{\eta-1}\right)\bar{\varepsilon}_2 + \varepsilon_2 \qquad (17)$$

Taking the condition that the skeleton curve (14) also passes through Point D, and substituting (15) to (17) into (14) leads to:

$$o_{\varepsilon 2} = -\frac{\sigma_D - o_{\sigma 2}}{\bar{\sigma}_2}\left(1 + \alpha\left|\frac{\sigma_D - o_{\sigma 2}}{\bar{\sigma}_2}\right|^{\eta-1}\right)\bar{\varepsilon}_2 + \varepsilon_D \qquad (18)$$

The skeleton curve (14) is now defined uniquely, with $o_{\sigma 2}$ and $o_{\varepsilon 2}$ stipulated by (16) and (18), respectively. If, in Fig.4(d), loading is continued in the negative direction without unloading at Point C, the hysteresis curve eventually meets the skeleton curve at Point B, and the further path traces on the skeleton curve. When unloading occurs at Point E on the skeleton curve [Fig.4(e)], the new hysteresis curve that governs unloading and reloading is defined by taking Point E as the new origin and also by increasing the yield stress by $\beta\,|\,\Delta\sigma_3\,|$ [from $\bar{\sigma}_1$ to $(\bar{\sigma}_1 + \beta\,|\,\Delta\sigma_3\,|)$], with $|\,\Delta\sigma_3\,|$ as the stress increment from the kinematic hardening bound specified at the last load reversal to the present state (Point E) [Fig.4(e)]. The stress of the origin of the corresponding skeleton curve and the stress of the other intersection of the hysteresis curve with the skeleton curve [Point F in Fig.4(e)] can be estimated in the same manner as in (7) and (8), the strain at Point F as in (9), the strain of the origin of the skeleton curve as in (10), and finally the skeleton curve is defined uniquely.

As detailed in this section, the basic ideas developed originally for the I-K bilinear model can be incorporated into the RO model relatively easily. It should also be noted that, as indicated in (5) to (10) as well as in (13) to (18), determination of all variables included in the skeleton and hysteresis curves, like $o_{\sigma 1}$, $o_{\varepsilon 1}$, σ_B, and ε_B, is explicit, not requiring any iterative computation, although the functions involve power forms. As in the I-K bilinear model, the I-K RO model can also be programmed easily by monitoring the stress state with respect to the kinematic hardening bound. As long as the stress remains within the bound, the rules enforced for the RO model can be used, and, only when the stress exceeds the bound, a new set of hysteresis and skeleton curves need to be constructed, and it can be done explicitly in consideration of the current state only.

Comparison Between Analysis and Test

The validity of the I-K RO model was checked against the test for which the I-K bilinear model was calibrated earlier. The values used for the five parameters included in the model were 54.3 MPa (in terms of the shear stress) for the initial yield stress, 50.0 GPa (in terms of the shear modulus) for the initial elastic stiffness, 1.0 for α, 15.0 for η, and 0.78 for β. These parameters were chosen by regression analysis so that the curves would match most closely to the initial two cycles and half [with the drift angle of 0.00227 (1/441)] in the experimental hysteresis. Figure 5(a) shows comparison of two hysteresis curves, one experimental and the other obtained from the I-K RO model. Correlation between the two curves is very satisfactory; growth of strength by strain-hardening is simulated very accurately, and gradual degradation in stiffness as well as Bauschinger effects are also traced with a satisfactory accuracy. The latter has been achieved thanks to the characteristics of the RO model. Good correlation observed here, however, is not entirely generic, because the model's parameters were selected in reference to a particular set of test data, and the accuracy of the model was checked only against that set of data. This type of comparison, which may be called interpolated compari-

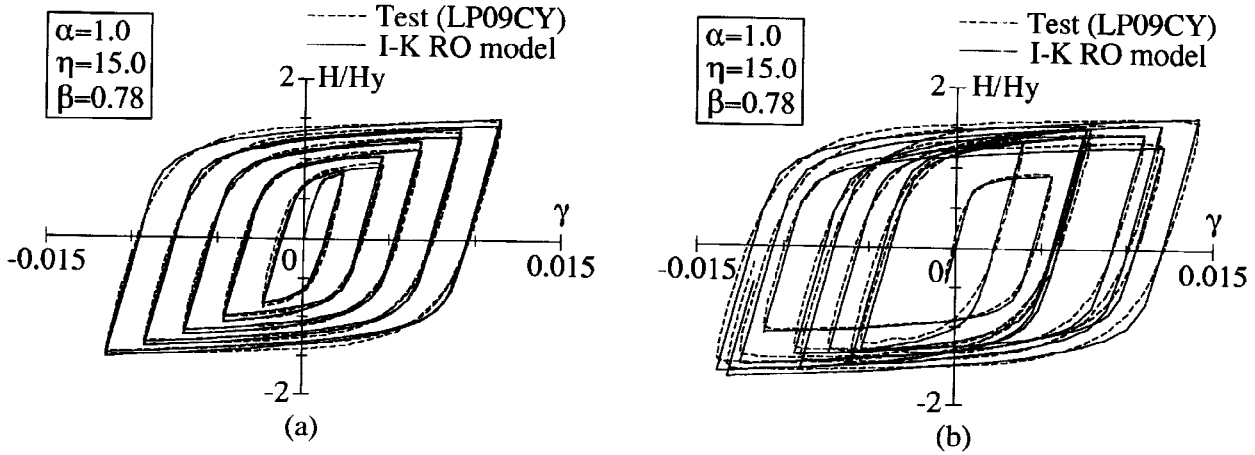

Fig.5 Comparison Between Experimental Hysteresis and Hysteresis Obtained from I-K RO Model : (a)Test LP09CY; (b)Pseudo-Dynamic Test

son, is useful as the initial step of examination, but, in the end, the ability of the model should be calibrated through extrapolated comparison, i.e., comparison with other data than the data that was used for determining the model's parameters. To this end, the model was used to simulate the hysteresis curves obtained from an earlier pseudo-dynamic test applied to another shear panel damper (Nakashima *et al.* 1994). For the five parameters used in the model, the values selected earlier were used again for ensuring extrapolated comparison. Figure 5(b) shows the comparison between the analysis and the test, demonstrating that the two hysteresis loops match each other very closely and that the model can successfully trace the experimental hysteresis that involves significant strain-hardening.

If associated parameters are selected adequately, the I-K RO model explicated in this section is deemed more accurate than the I-K bilinear model, because the I-K RO model is able to duplicate the behavior of gradual stiffness degradation (rather than sharp yielding) characteristic to shear panels made of low-yield steel.

I-K RO Model for Simulating Hysteresis Involving Very Large Deformations

Figure 6(a) shows comparison between the experimental hysteresis and the one simulated by the I-K RO model, this time up to a large deformation (0.06 in drift angle), indicating that the analytical curves somewhat overestimate the shear forces. Figure 6(b) shows the experimental shear force versus drift angle curves drawn for each half-cycle of the hysteresis curve from an extreme displacement to the next extreme displacement, with the initial extreme displacement shifted to the origin. For negative loading, the negative signs were converted to positive for both the shear force and the drift angle. Furthermore, those curves are drawn with halved coordinates. The experimental curve obtained for the same shear panel but tested in one-way monotonic loading is also plotted in this figure. Comparison between half-cycled curves in large deformation amplitudes and the curve obtained from the one-way loading test suggests that the degree of strain hardening is somewhat smaller in large deformation amplitudes, and it is for this reason that the model overestimates the shear forces in these amplitude ranges.

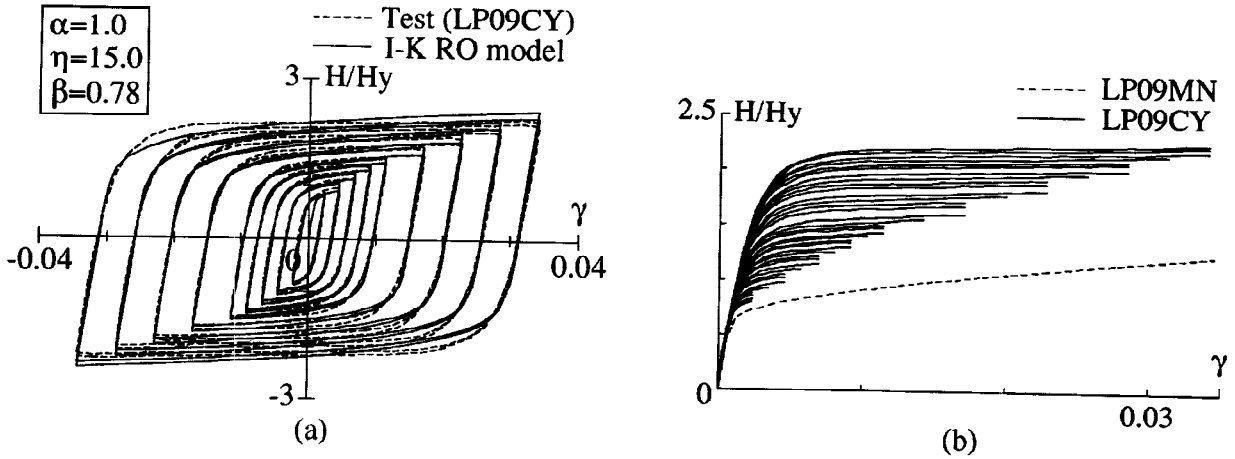

Fig.6 Shear force vs. Drift Angle Relationship up to Large Deformations: (a)Comparison Between Experimental Hysteresis and Hysteresis Obtained from I-K RO Model (from Test LP09CY); (b)Comparison Between Cyclically Loaded Test (LP09CY) and Monotonically Loaded Test (LP09MN)

Inability of handling the changes in the hysteresis shape is the limitation of the I-K RO model. To overcome this limitation, a modified version of the I-K RO model is devised. In consideration of the fact that the degree of strain hardening decreases with the increase of deformations (and shear forces) and also that in the RO model the strain hardening becomes smaller with the increase of the parameter α, in the modified model this parameter is adjusted in accordance with the yield stress value. Two sets of α and yield stress values are determined in reference to Fig.6(b), one for the experimental curve given under one-way loading (representing the virgin curve) and the other for the half-cycled curve with the largest deformation, and linear interpolation is assumed for α values in intermediate deformation ranges.

Figure 7(a) shows the analytical hysteresis curves obtained from this model together with the corresponding experimental hysteresis curves, demonstrating that this model can trace experimental hysteresis not only in small to medium ranges of deformation but in large deformations as well. In this simulation, the initial elastic stiffness and initial yield stress were set at 48.4 GPa (in terms of the shear modulus) and 51.2 MPa (in terms of shear stress), and the other three parameters: β, η, and α_0 (the initial α value), were chosen by regression analysis applied for the experimental curves of the first two and a half cycles. Figure 7(b) is a comparison

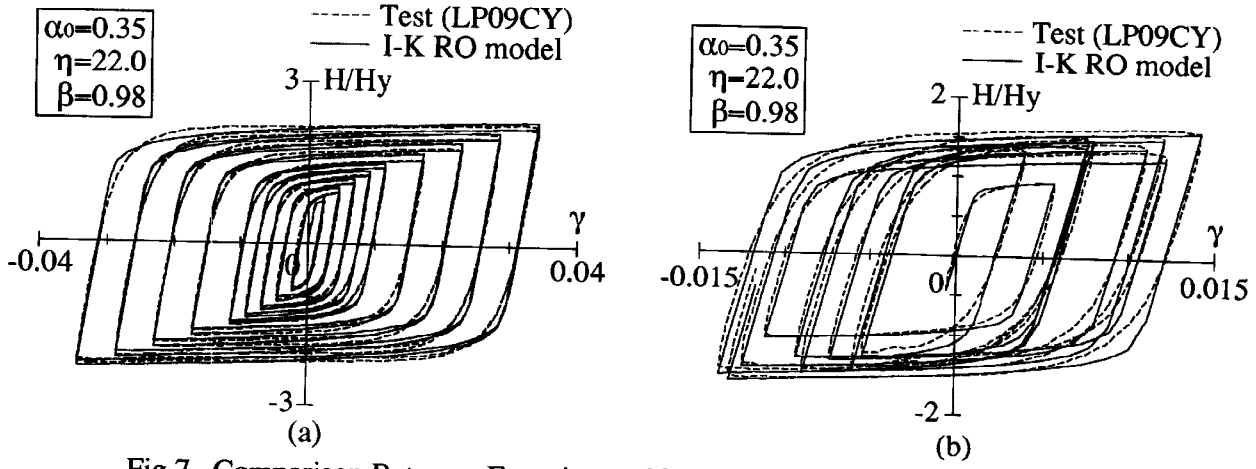

Fig.7 Comparison Between Experimental Hysteresis and Hysteresis Obtained from Modified I-K RO Model: (a)Test LP09CY; (b)Pseudo-Dynamic Test

between the hysteresis curves obtained from the pseudo dynamic test and the hysteresis curves obtained from this model. Again, good correlation is achieved, verifyting that this model maintains the ability to simulate the hysteretic behavior that would be generated under earthquake loading condition.

CONCLUSIONS

This paper presented an analytical model that can simulate the hysteretic behavior of dampers made of low-yield steel. A summary of the paper is as follows:

1. A simple model, called the I-K bilinear model, was introduced, and its ability to simulate the hysteretic behavior of shear panel dampers was calibrated.
2. It was indicated that the ideas embedded in the I-K bilinear model can easily be applied to hysteresis models other than the bilinear model, and a model based on the Ramberg-Osgood functions (designated as the RO model) was chosen, and a new model, called the I-K RO model, was devised. Comparison between analytical and experimental curves verified that this model is also capable of accurately simulating significant strain-hardening behavior involved in shear panels made of low-yield steel. Furthermore, this model was found to be able to trace gradual stiffness degradation exhibited in the experimental hysteresis curves.

REFERENCES

Izumi, M. et al. (1992). Low cycle fatigue tests on shear yielding type low-yield stress steel hysteretic damper for response control, Part 1 and 2. *Proceedings of Annual Meeting of the Architectural Ins. of Japan*, Tokyo, Japan, 1333-1336 (in Japanese).

Hill, R. (1950). *The mathematical theory of plasticity*. Oxford.

Jennings, P. C. (1964). Periodic response of a general yielding structure. *Journal of Engineering Mechanics Division*, ASCE, **90(EM2)**, 131-166.

Nakashima, et al. (1994). Energy dissipation behavior of shear panels made of low-yield steel. *International Journal of Earthquake Engineering and Structural Dynamics*, **23**, John-Wiley & Sons, 1299-1313.

Nakashima, M., Akazawa, T., and Igarashi, S. (1995). Pseudo-dynamic testing using conventional testing devices." *International Journal of Earthquake Engineering and Structural Dynamics*, **24**, John-Wiley & Sons, 1409-1422.

Nakashima, M. (1995). Strain-hardening behavior of shear panels made of low-yield steel. I: test. *Journal of Structural Engineering*, ASCE, **121(12)**, 1742-1749.

Nakashima, M., Akasawa, T., and Tsuji, B. (1995). Strain-hardening behavior of shear panels made of low-yield steel. II: model. *Journal of Structural Engineering*, ASCE, **121(12)**, 1750-1757.

Prager, W. (1956). A new method of analyzing stresses and strains in work-hardening plastic solids. *Journal of Applied Mechanics*, ASME, 493-496.

Tamai, H., et al. (1991). On hysteretic damper using low-yield stress steel plate installed in K-braced frame, Part 1 and 2. *Proceedings of Annual Meeting of the Architectural Ins. of Japan*, Tokyo, Japan, 1447-1450 (in Japanese).

Yamada, M. and Tsuji, B. (1965). Stress-strain behavior of structural steels. I: combined isotropic and kinematic hardening model. *Transactions of the Architectural Institute of Japan*, Tokyo, Japan, **270**, 17-22 (in Japanese).